CHAPTER ONE

1.1 INTRODUCTION

The ionosphere is a region of significant interest due to its numerous complexities. Even though people have greatly improved their use of the ionosphere's features over the past century, there is still more to learn about the physical and chemical changes that have occurred in this area of the earth's atmosphere. Total Electron Content (TEC) is a parameter utilized to examine the ionosphere. . It is a significant ionosphere descriptive quantity. The integral of electron number density along the line of sight path from the satellite to the receiver is called TEC, and it can vary significantly (Rastogi et al, 1990).The TEC is significant in helping us to understand the short and long term changes of the upper atmosphere during major phenomena caused by factors like solar activities, geomagnetic storms and meteorological influence e.g (Forbes et al; 2000). Among the various phenomena in the ionosphere, TEC is responsible for time delay, which produces range errors in the GPS radio signal of a satellite to ground radio communication. At the same time, the perturbations in the GPS signals can be used as scientific information to investigate the Ionospheric variability. Since the signal from the satellite to the receiver must travel via the ionized layer, these alterations in the ionosphere have an impact on modern technologies including communication systems, navigation systems, and surveillance systems (Bagiya et al., 2009). Consequently, a comprehensive characterization of the ionosphere is essential to improve the efficacy of ionospheric models (Bilitza, 2000). Studying the ionosphere's characteristics, such as its fluctuations according to the solar cycle, season, and time of day, is therefore essential.

The plasma density irregularities, which encompass a wide range of scale sizes (from a few cm to a few hundred km), are referred to as the Equatorial spread F (ESF) (Paznukhov et al., 2012). Plasma depletions, commonly referred to as Equatorial plasma bubbles (EPB's), are the irregularities of the largest scale sizes (up to a hundred km) that are associated with the ESF in which the plasma density can be lowered up to three orders of magnitude compared to the background (Dashora and pandey, 2005). TEC measurements have been used to diagnose the dynamics that drive the formation of plasma depletions. The presence of plasma irregularities within these depletions disrupts satellite communication by scattering radio signals that pass through them. The origin and variability of the plasma density depletions in relation to the variability of the ionospheric total electron contents have been well documented (Valladares et al., 2004; Dashora and Panday, 2005). Rapid changes in electron density caused by space-weather disturbances may also cause severe TEC depletions. Sudden reductions in TEC that are observed in the night time low latitude F region have been linked to the Equatorial origin of the plasma density depletions (Valladares et al., 2004). During day time, the E region dynamo electric field give rise to an upward electrodynamics E X B drift that causes the f- region plasma to diffuse downward along geomagnetic field lines under the influence of gravity and pressure and pressure gradients, resulting in the equatorial ionization anomaly at about 15^0 magnetic latitude on either side of the equator. After sunset, plasma densities and dynamo electric fields in the E- region decrease, and the anomaly begins to fade, and at this local time a dynamo electric field develops in the

F- regions (Rama Rao et.al., 2006a; Valladares et.al., 2004). Polarization charges, set up by the conductivity gradients at the terminator, enhance the east ward electric field for about an hour after sunset. With the decreased ionization density in the E - region after sunset, vertical plasma density gradients form in the bottom side of the F layer, resulting in the upward density gradients opposite in direction to the gravitational force. Such a configuration is known as the Rayleigh-Taylor (RT instability, and allows plasma density irregularities to occur (Rama Rao et al., 2006a; 2007; Paznukhov et al., 2012). These irregularities can grow to become large ionospheric depletions, resulting in equatorial plasma bubbles (EPBs). Ionospheric irregularities may be due to geomagnetic storms, which can affect the ionsosphere and hence modify the ionospheric parameters therein (Rama Rao et al., 2009; Basu et al., 2007). A highly dynamic ionosphere affects both space – based systems and ground based systems leading to wastage of economic resources.

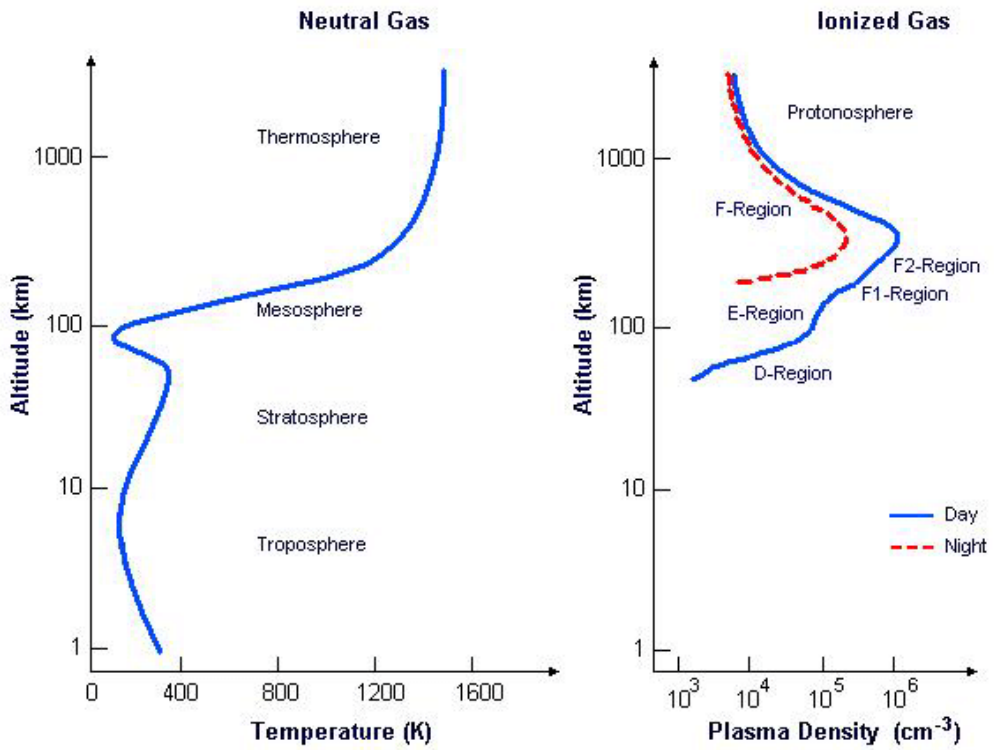

Figure 1.1: Layers of the neural Earth atmosphere with temperature and the layers depending on the ionospheric electron density profiles. Source: (Rishbeth and Garriot 1969).

1.2 AIM AND OBJECTIVES

The aim of this study is to investigate the TEC variation dependence in the low latitude stations Marshal Island and Peru during solar cycles 23. (August 1996 – December 2008).

CHAPTER TWO

2.1 Ionospheric Error

The atmosphere containing ions is made up of weakly ionized plasma of electrons and ions that are mainly caused by the presence of ionizing solar radiation. The electron density integrated in a vertical column with a cross-sectional area of one square meter is known as the total electron content. The two main effects of the ionosphere are the group delay of pseudorange and the carrier phase advance. GPS signals are affected as they pass through the ionosphere, resulting in range errors, the magnitude of which depends on the frequency of the signal and the density of free electrons along the signal path.

The phase advance and group delay are equal in magnitude and opposite in sign. The pseudorange ionospheric group delay ranges 1 m 100 mm (Shrestha, 2003). GPS ionospheric range errors are a function of the TEC along the signal path and the signal frequency.

The variation of TEC and ionospheric effects on GPS signals depends on different ionospheric characteristics. The electron density is directly proportional to the rate of ionization, which depends on the level of solar radiation, and solar wind characteristics (in auroral and polar regions). In the day time, solar radiation is high and creates free electrons; the electrons recombine with ionospheric ions in the night time local time sector. The highest number of free electrons occurs at approximately 14:00 local time, and a secondary maximum may occur 22:00 local time in the equatorial region. The TEC also depends on the season and geographic location. Electron densities are highest at spring equinox and two maxima in TEC are located at ± 20 degrees magnetic latitude.

Electron densities also increase by a factor of 3 in the period of solar maximum. When the sun is at its greatest, there are more sunspots than when it is at its minimum. Because of changes in temperature and recombination processes, TEC in mid-latitudes deviates by roughly 25% from monthly mean values. These numbers indicate the extremes of observed values in the Earth's ionosphere, and the TEC measurement can fall between 1016 and 1019 TECU (Klobuchar, 1996). As a dispersive medium, the ionosphere causes transio-ionospheric signals, like GNSS signals, to experience a frequency-dependent temporal delay. Since ionospheric-induced error has been identified as one of the biggest and most variable causes of error for GNSS applications, this could impair or even interfere with satellite-based communication operations (Oladipo and Schuler, 2012; Bagiya et al., 2009).The delay in the ionosphere, a dispersive material, depends on the radio signal's frequency. Using the following formula for the medium's refractive index by Appleton and Hartree (Klobuchar, 1996), one can describe the propagation effects on a radio wave passing through the ionosphere.

$$n^2 = 1 \; {}_{1-iz} \frac{X}{\frac{Y^2T}{2(1-X-iz)}} \pm \left[\frac{Y^2T}{4(1-X-iz)^{\;2}} + \; {Y_L}^2\right] \tag{2.1}$$

Where

$$\mathrm{X} = N_e \frac{E^2}{\varepsilon m w^2}, \; Y_L = \left(\frac{f_{H cos\theta}}{f}\right), \; Z = \frac{\theta}{w} \quad and \; w = 2\pi f \tag{2.2}$$

f = frequency of the signal

E = electron charge

$\varepsilon_0 = permititvity \; of \; free \; spac,$

m= mass of an electron,

$$\theta = angle \; of \; the \; ray \; with \; respect \; to \; the \; Earth's magnetic \; field$$

$N_e = ionospheric \; electron \; density$

ν = *electron – neutral collision frequency*

$f_H = electron\ gyro\ frequency$

With an accuracy of better than 1% using the following approximation, the refractive index of the ionosphere can be determined.

$$n = 1 - \frac{X}{2} \tag{2.3}$$

The ionospheric group delay can then be determined using the following equation (Lachapelle et al., 2002).

$$\Delta_t = \frac{40.3}{f^2}\ TEC \tag{2.4}$$

$\Delta_t = Ionospheric\ time\ delay$

f = frequency of the signal,

c = speed of light

TEC = Total Electron Content

$$\Delta\emptyset = \frac{1.34 \times 10^{-7}}{f}\ TEC \tag{2.5}$$

$$\Delta\emptyset = Phase\ shift\ due\ to\ the\ ionospheric\ refractive\ index$$

Ionospheric scintillations are rapid fluctuations in the phase and amplitude of signals caused by electron density irregularities in the ionosphere; the effects of ionospheric scintillations may be observed as the loss of phase lock due to lower signal strength or due to Doppler shift outside the bandwidth of the phase lock loop. Other effects of the ionosphere include absorption, faraday's rotation or change in plane of polarization, Doppler shift, refraction or bending of the radio waves, Absorption, and scintillation. The ionospheric effects can be virtually eliminated using dual frequency data to correct the

pseudorange measurements. The ionospheric correction removes the first order ionospheric effect, but it increases the noise on the ionospherically corrected pseudorange. The ionospheric correction can be applied on the L1 carrier phase at a given epoch using dual frequency carrier phase observations and known carrier phase ambiguities for L1 and L2. However, the differential ionospheric delay delay correction can be applied using both L1 and L2 carriers without knowing the ambiguities in a float ambiguity positioning approach. The broadcast ionospheric model removes over 50% of the ionospheric delay at mid- latitude regions. The wide areas DGPS ionospheric grid model may also be used to estimate ionospheric delays for individual satellites at a user's location (Shrestha,2003).

2.2 THE EARTH IONOSPHERE AND ITS VARIATION

The earth's upper atmosphere contains a partially ionized area known as the ionosphere. It comprises of ions and free electrons, usually in equal amounts, in an electrically neutral medium (Hargreaves, 1995). The ionosphere has a range of between 60 to 1000 kilometers. Solar radiation, including X-ray and extreme ultraviolet (EUV) radiation, is the primary cause of ionization. Another source of ionization at the topside ionosphere is particle precipitation from the magnetosphere at the aurora latitudes, which causes intense particle collisions that cause photoionization (Kelley, 1989). The processes explained above lead to the production of plasma, which undergoes chemical reactions with the neutrals, diffuses due to the gravitational force and pressure gradients, and it is transported through neutral winds and electric field under the influence of the Earth's magnetic field.

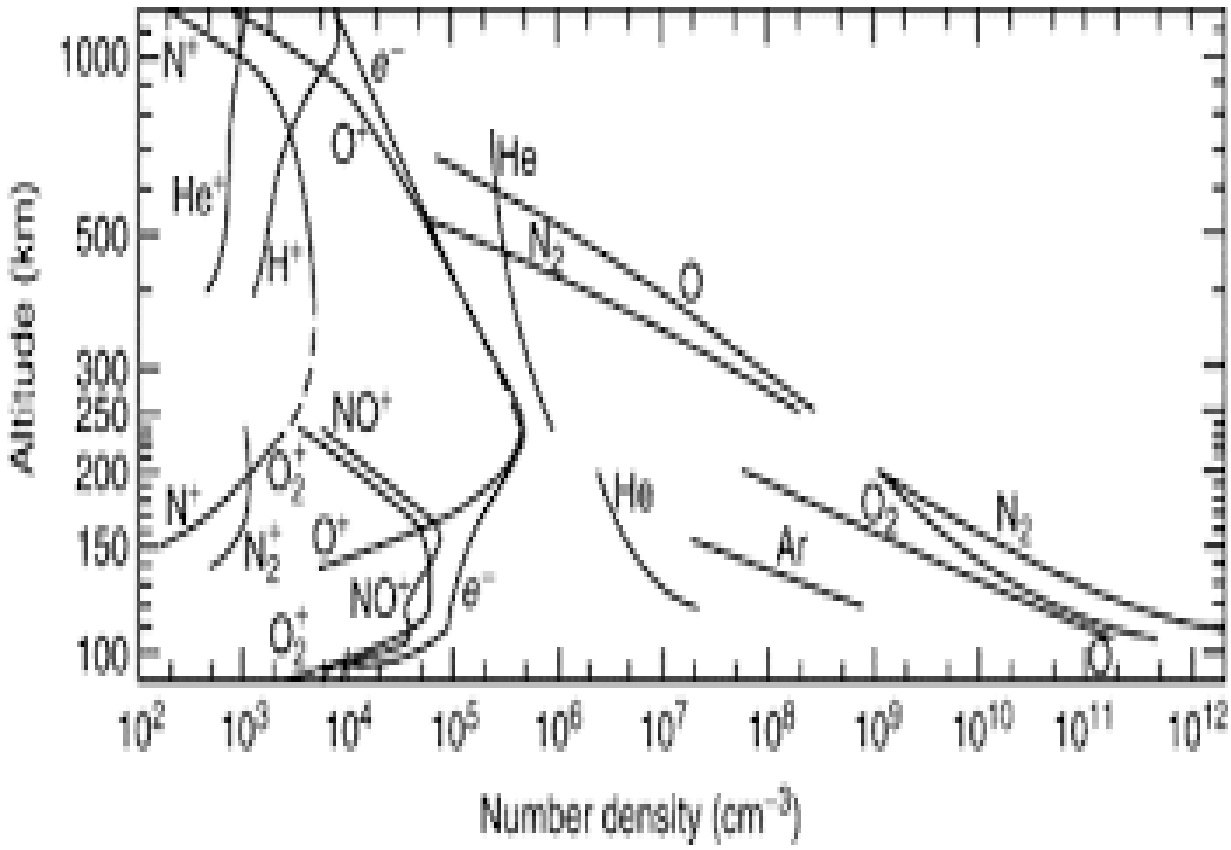

Figure 2.3: Typical Vertical profile of the electron ions and neutral densities in the Middle latitude. Source: (Kelley, 1989).

As a result of the altitude variations in the atmospheric neutral composition and the production rate with altitude, the plasma density in the ionosphere has vertical layer structures, which are denoted by the D, E, F layers. These layers are controlled by different physical and chemical process and have different composition of ions. The D and E regions are dominated by more molecular ions (O2+, N2+, NO+). The recombination rates at these regions with electrons is higher and hence lead to the disappearance of both layers after sunset. On the other hand, the F region is composed mostly of atomic ions (O+ and H+). The recombination rate with electron is much more

lesser and therefore part of the layer is sustained during the night. The maximum electron density is obtained in the F region. Above the F2 peak is the topside ionosphere, where diffusion dominates and the chemical composition is H+ and He+. The results of the processes of ionization and ions loss, along with the dynamics of Ionospheric regions, determine the electron density profile with different behaviour's in their vertical structure depending on ionizing radiation, seasons, latitude as well as differences between the day and night. The following major variations are briefly discussed

2.2.1 **Diurnal variation**

The rotation of the Earth is the cause of the day-night changes. Because there is no radiation source present, recombination rates are higher at night, resulting in significantly lower electron densities than during the day. The atmosphere of the earth lags two hours behind the rotation of the solid earth, hence daytime electron concentrations usually peak two hours past local noon (Opperman, 2007).

2.5.2 **Seasonal variations**

The sun is vertically over several geographic areas at different periods of the year. On solstice days (21 December, 21 June), the sun is vertically above viewers at the equator at equinox midday (March 21, Sep 23) and vertically above observers at the tropics of Capricorn and Cancer. Higher electron density concentrations are seen at these sites on these dates compared to other locations because vertical irradiation from the sun causes higher ionization rates (Opperman, 2007).

2.5.3 Spatial variations

Unlike diurnal and seasonal variations, the sun's position relative to the atmosphere plays a significant role in spatial variations of ionospheric densities (Opperman, 2007).

2.3 FORMATION OF THE IONOSPHERE

In most parts of the lower atmosphere, the constituent molecules are in combined state and remain electrically neutral. In the region extending from a height of about 50km to over 600km, however solar radiation (main ultraviolet light) is so intense that when it strikes the gas molecules they split (that is, they become ionized) and electron are set free. The result is the production of positive ion (a molecule that has lost an electron) and a free electron. Since this process requires solar radiation, major production of electrons occurs in the day light hemisphere of the ionosphere. Where a free electron combines with a charged ion, a neutral particle is usually lighter and more freely moving electrons (Adeniyi 2008). At the outer of the earth environment, power density (solar constant) reaches a value of 1370w/m^2, this intense level of radiation is spread over a broad spectrum ranging from radio frequencies through infrared (IR) and visible light to X-rays. Solar radiation at the ultraviolet (UV) and shorter wavelength is considered to be "ionizing" since photons of energy at these frequencies are capable of dislodging an electron from neutral gas atom or molecule during a collision. The conceptual drawing below is simplified explanation of this process:

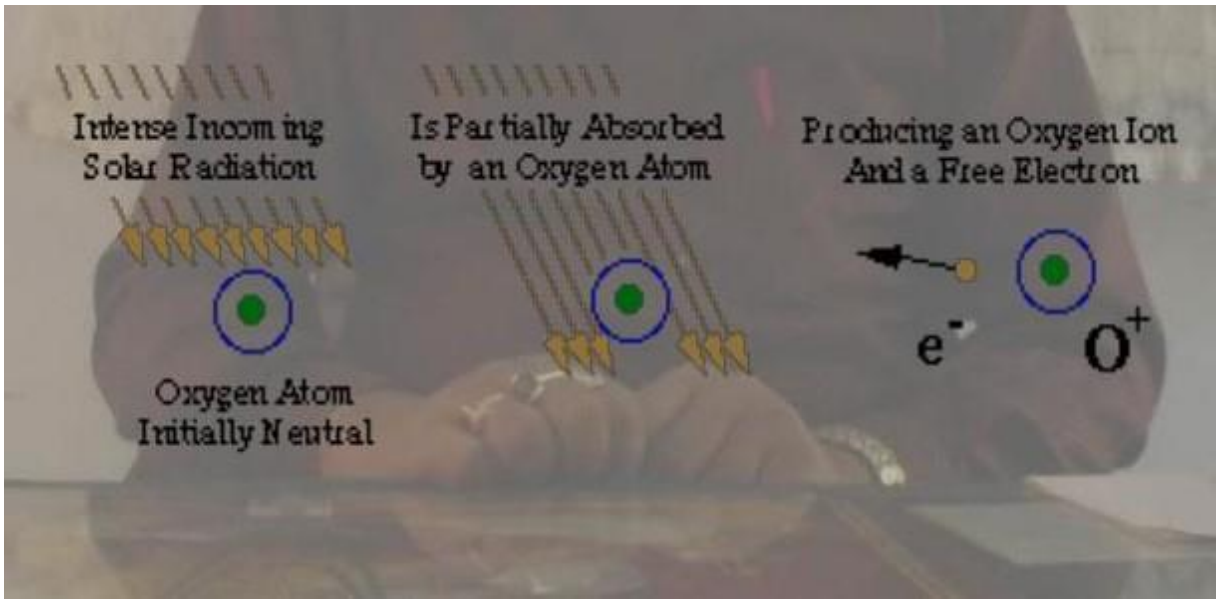

Figure: 2.1: Conceptual image of the formation of the ionosphere

Ionizing solar radiation is incident on a gas atom (or molecules). In the process, part of this radiation is absorbed by the atom and a free electron and a positively charged ion are produced. (Cosmic rays and solar wind particles also play a role in this process but their effect is minor compared with that due to the sun's electromagnetic radiation). At the highest levels of the earth's outer atmosphere, solar radiation is very strong but there are few atoms to interact with, so ionization is small. As the altitude decreases, more gas atoms are present so the ionization process increases. At the same time, however, an opposing process called recombination begins to take place in which a free electron is "captured" by a positive ion if it moves close enough to it. As the gas density increases at lower altitudes, the recombination process accelerates since the molecules and ions are closer together. The point of balance between these two processes determines the degree of "ionization" present at any given time.

2.4 **IONOSPHERIC LAYERS**

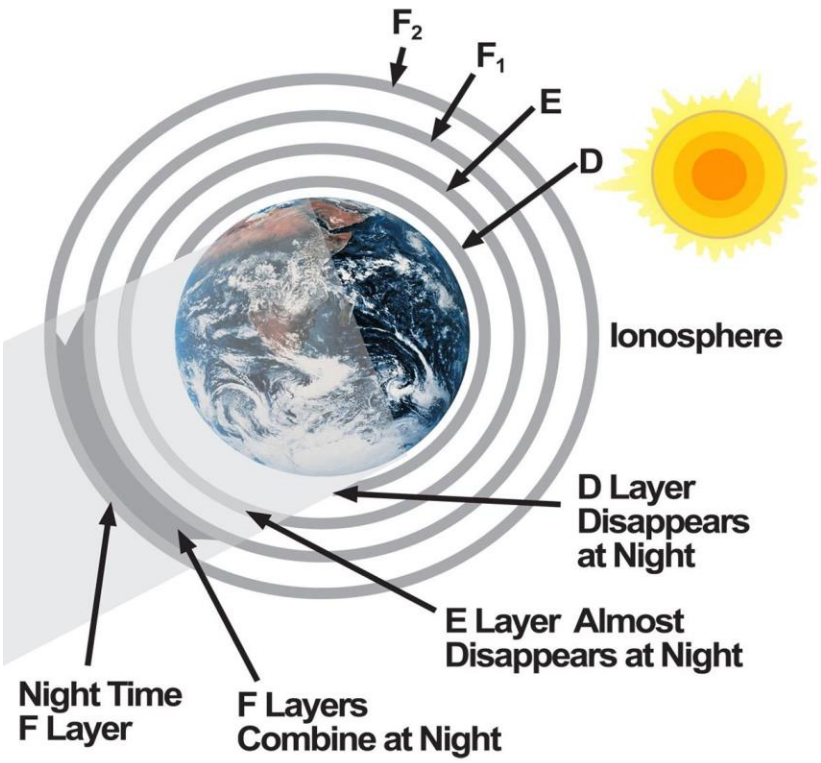

Figure 2.2: illustration of the layers of the Earth – ionosphere

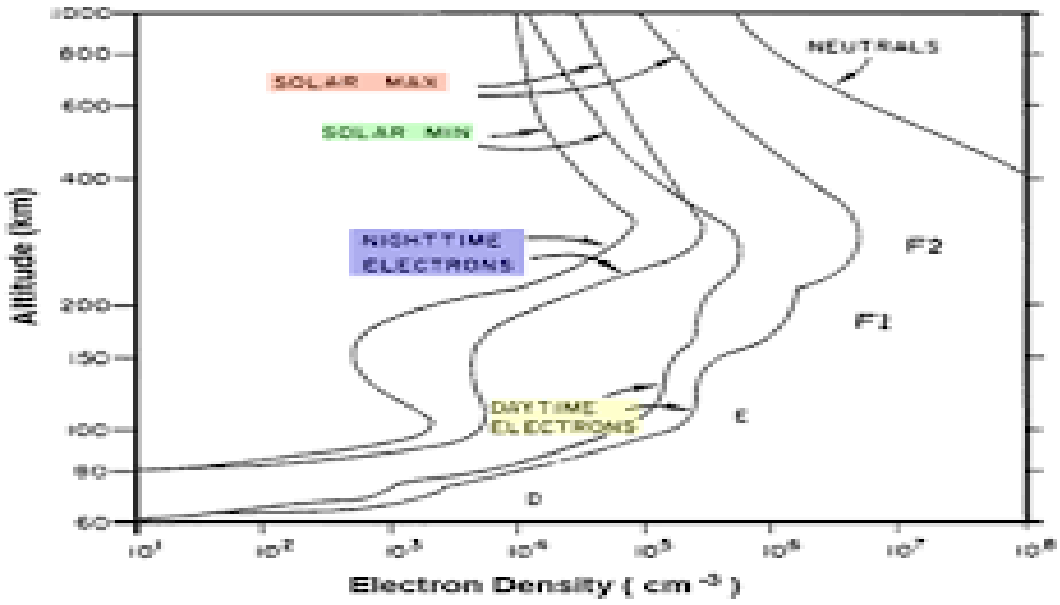

Figure 2.3: Ionospheric layers and there solar minimum and maximum

The ionosphere is a partially ionized region of the earth's upper atmosphere. It comprises of free electrons and ions, generally in equal numbers, in a medium that is electrically neutral (Hargreaves, 1995). It is an important region that plays a significant role in global communication and navigation systems, as well as space weather. The total electron content (TEC) of the ionosphere, which is a measure of the number of free electrons in a given area, is influenced by various solar ionizing indices, the correlation between TEC and these indices in different regions of the ionosphere during solar cycle 23 is an important area of research. This paper aim to examine the TEC variation in the low equatorial region of the ionosphere during solar cycle 23.

D Layer: located at the bottom of the ionosphere up to approximately 90 km height. This region presents a complexity in chemical and photochemical processes which may be characterized by low density and high ionization collisions frequency of electrons with

ions and neutral particles. There are three ionization sources in this region, these being X-rays, cosmic rays and Lyman –α radiation. The regions dominates by more molecular ions (O2+, N2+, NO+). The ionization of this region is however very low ranging from 107 to 1010e/m3.

E Layer: Situated between 90-140 km high, is characterized by increased electron density between 90- 110 km. This region of high conductivity is very low important due to the presence of ionospheric electrical currents and the interaction of these currents with the earth's magnetic field. The main sources of ionization are weak X- rays radiation, solar Lyman – β and EUV. At mid and low latitudes, the probability of occurrence of these Es layers is major during the summer daytime hours. While at high- latitudes the probability of occurrence is more pronounced at night time hours.

F Layer: located approximately between 150-1000 Km height. Its main sources of the ionization are EUV Lines and Lyman continuous of hydrogen. The dominant ion is O+. The F region can be characterized by two other layers, F1 and F2. In the equatorial region may create a third layer named F3. The layer F1 is defined based on an inflection or a peak in the curve electron density around 180 km. F2 layer is located in vicinity of the peak electron density (300-400 km), and it is the region with higher ionization density of the ionosphere. Its formation is predominantly dependent of the winds and its concentration varies with solar activity.

The highest concentration of free electrons can be observed during the day, especially during local noon. During the night, this concentration decreases, but the layers remains due to low recombination of ion with neutral and wind transport effects. The equatorial

meridional wind plays an important role in the night-time F layer density maintenance. In addition to the variation of the plasma density with altitude, the ionosphere also shows important changes with time of day, latitude, longitude, season, solar activity and geomagnetic activity. Latitudinal variation has a distinctive behavior due to the geometry of the earth's field lines. Hence the ionosphere can be classified by three latitudes controlled by different physical processes: the low and equatorial, middle and high (aurora) latitude regions.

2.5 MAJOR GEOGRAPHIC REGIONS OF THE IONOSPHERE

The three major regions of the global ionosphere are: the equatorial regions, Mid – latitude and High- latitude (See Fig.2.4).

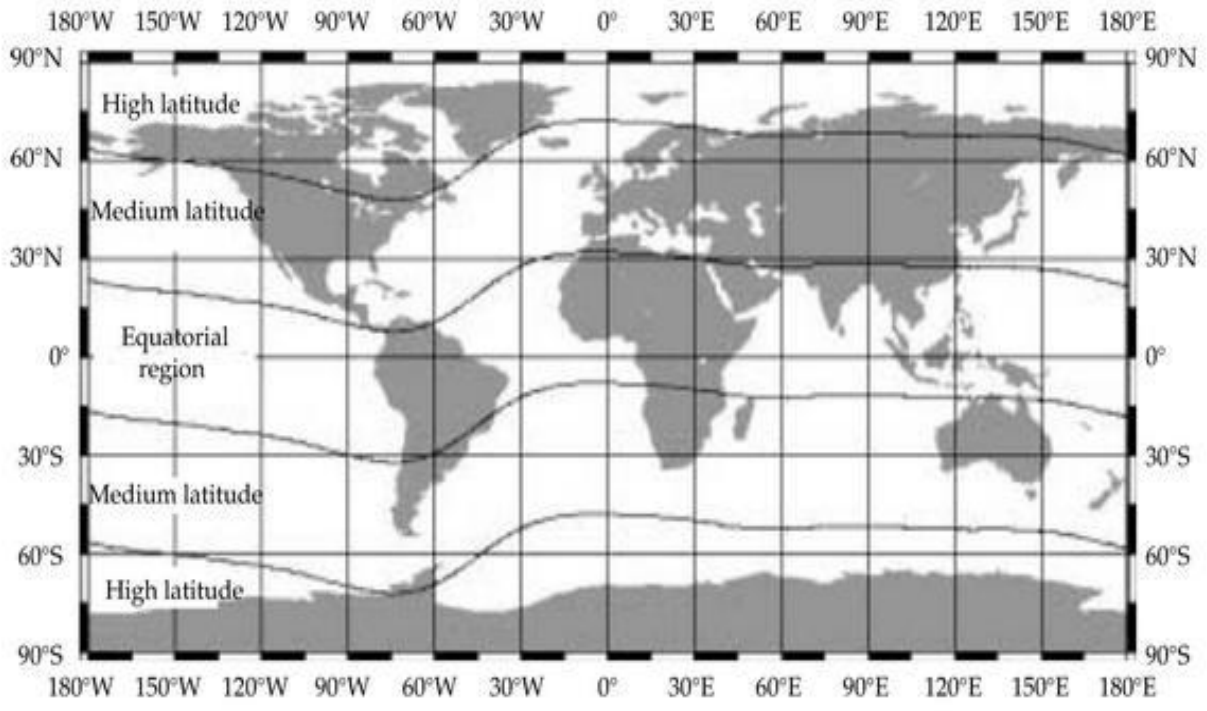

Figure 2.7: Major geographic regions of the ionosphere (Bishop et al.,1991).

2.5.1 LOW OR EQUATORIAL REGION

The equatorial ionosphere is the region under the geographic latitudes (0 - ±30°) of the geomagnetic equator), due to the near horizontal orientation of the geomagnetic field lines of the magnetic equator, possesses peculiar characteristics such as equatorial ionization anomaly (EIA) and fountain effect among others. These attributes make the equatorial ionosphere more challenging to satellite signals. Ionospheric irregularities have been observed to be a regular occurrence at the equatorial latitudes during post sunset periods even at quiet periods. These irregularities, (according to Oladipo et al., 2014, Chu et al., 2013, de Paula et al., 2003) are sources of degradation and fading of trans-ionospheric signals traversing the equatorial ionosphere. The equatorial and low latitude ionosphere represents considerably different behavior in comparison to mid and high latitude ionosphere. The main reason behind this is that here the Earth's magnetic field lines are almost horizontal, and the Earth's atmosphere is most exposed to Sun's ionizing radiation. And hence, according to Lorentz force, the charged particles move readily along the field lines than perpendicular to it.

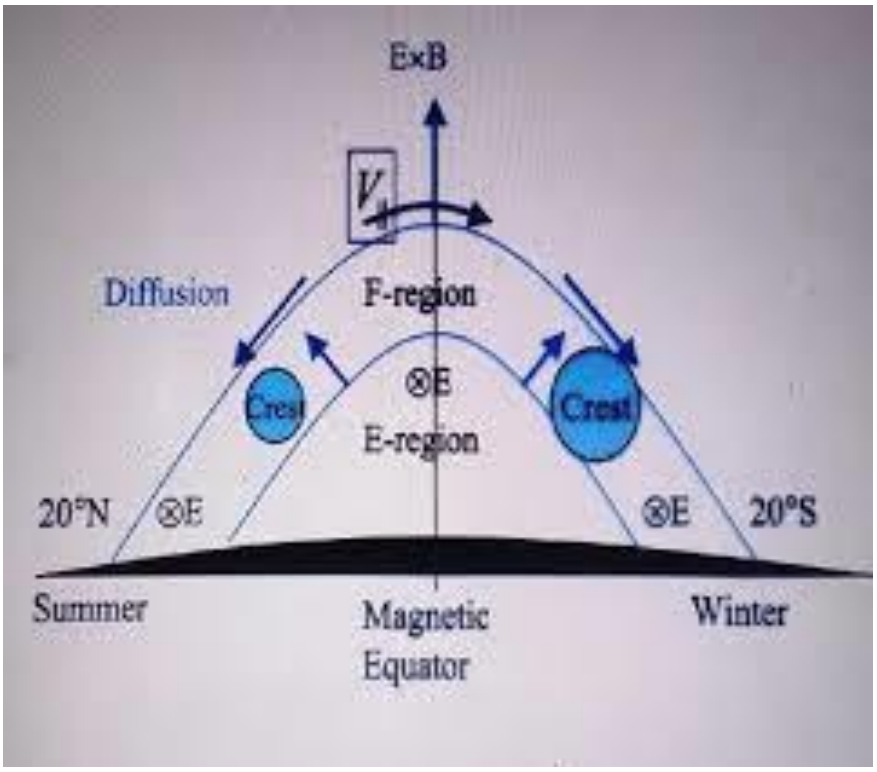

Figure 2.4: Asymmetry of the equatorial ionization anomaly. E denotes an eastward electric field and B is the northward geomagnetic field. (Source: Anderson and Roble (1981)).

2.6 **TOTAL ELECTRON CONTENT**

An effective method for researching the ionosphere is the Global Positioning System, a satellite-based navigation system that transmits and receives radio signals. According to Strangeways and Walsh (2007), the significance of the ionosphere stemmed from its impact on radio waves and, consequently, on the transmission of electromagnetic waves by satellite-based navigation systems. In contrast to the time it takes for a signal to propagate over free space, GPS radio transmissions take longer to travel through the ionosphere because they are slowed down. Positioning requires consideration of this

effect, which is known as the propagation delay (Perevalova, 2008). Ya'acob et al. (2009) expressed the group delay's absolute value in terms showed below

$$/\emptyset.g = \frac{80.6}{2f^2}\int Nedh \quad (2.6)$$

Parameters involved are defined as follows:

$/\emptyset.g = Group\ delay\ of\ radio\ signal\ propagation$

$Ne = Number\ of\ electrons\ at\ distance$

$f = System\ operating\ frequency\ in\ MHz$

Total Electron Content is defined as the total number of electrons integrated along the path from the satellite to the receiver. Given as,

$$TEC = Nedh \quad (2.7)$$

where:

$$TEC = Total\ Electron\ Content, measured\ in\ unit\ of\ (TECU) = 10^{16}\ e/m^2$$

$$Ne = electron\ density\ along\ the\ ray\ paths\ from\ satellite\ to\ reciever$$

TEC is a parameter that has an ionosphere effect on radio systems, in many applications such as radio links between satellites and ground. TEC plays a role in modern communications technology, in navigation and surveillance, where propagation departs from free space conditions in various ways with significant consequences for the accuracy and reliability of the service (Jakowski, 1996). Total Electron Content is a parameter of the ionosphere that is widely used in studies of the near-earth plasma environment, which is an indicator of ionospheric variability that produced most of the effects on GPS signals. The propagation delay could characterise by substituting TEC into equation (2.6). Which would then yield (Ya'acob et al, 2009).

$$/\emptyset.g = \frac{40.3}{f^2}TEC(m) \quad (2.8)$$

$$/\emptyset.g = \frac{40.3}{cf^2} TEC(s) \quad (2.9)$$

Defining the parameters, they are:

$/\emptyset.g = Group\ delay\ of\ radio\ signal\ propagation$

$TEC = Total\ electron\ content\ in\ e/m^2$

$f = System\ operating\ frequency\ in\ MHz$

$c = speed\ of\ light\ which\ has\ value\ of\ 3 \times 10^8\ m/s$

The position correction, also known as the signal propagation delay, is really proportional to the line integral of the distribution of free electrons along the signal's journey from the satellite transmitter to the receiver. For instance, the changes that take place during ionospheric storms, ion composition changes, and space weather effects on telecommunications are just a few of the phenomena that can be studied using this information. It can also be used to determine the electron density distribution in the earth's ionosphere and plasmaphere mean study behavior of the ionosphere and magnetosphere. This information can be used to correct for the propagation delay in GPS signals (Pedatella et al., 2009).

Therefore, one of the most crucial techniques for examining the earth's ionosphere and plasmaphere is TEC measurements, which are performed using transionospheric radio transmissions. A set of TEC measurements, however, are not maps of the electron density distribution or structure; rather, they are only a collection of line integrals of free electron density (Yizengaw, 2004).

2.6.1 Slant and Vertical TEC

In general, there are two types of TEC Slant (STEC) and Vertical TEC (VTEC). Where Slant TEC (STEC) is defined by the total electron density along the ray path between

transmitter and receiver at angles deviating from the radial direction with respect to the Centre of the earth, or define as a measure of the total electron content of the ionosphere along the ray path from the satellite to the receiver, represented in Figure (2.8) as the quantity T_s or STEC. The slant total electron content, is along ray path 1 between a GPS satellite (T_X), and a ground based receiver (R_X) can be written as in equation (2.10) and (2.11) (Liu et al., 2004):

$$TEC_s = \int_{RX}^{TX} Ne\ dh = \frac{f^2}{40,3} \int_{RX}^{TX} (n^{-1} - 1) dh \quad (2.10)$$

$$TEC_s = \frac{f^2}{40,3} \int_{RX}^{TX} \left[\left(\sqrt{1} - \frac{f^3 N}{f^2}\right)\right] \exp - 1\ dh \quad (2.11)$$

where

Ne is the electron density in e/m^2, n denotes the refractive index, and f and f_N represent radio wave and plasma frequency in MHz, respectively'

Vertical TEC (vTEC) is normally given from the surface of the earth and up enables TEC to be mapped across the surface of the earth, represented in Figure (2.8) as the quantity or vTEC.

The I –axis stands for the receiver to satellite direction. Equation (2.16) is to convert slant TEC (STEC) to Vertical TEC (VTEC).

$$VTEC = STEC\ (\cos x^1) \quad (2.12)$$

where

STEC = value of slant TEC,

x^1 = The difference between 90^0 and zenith angle (90^0 - x).

2.6.2 **Total Electron Content (TEC) Calculation**

The GPS signal velocity through the ionosphere is directly related to the total electron content (TEC), which is the number of electrons in a cylinder with a cross sectional area of $1m^2$ connecting the satellite to the GPS (Misra and Enge, 2006; Kaplan and Hegarty, 2006).

$$TEC = \int_{satellite}^{user} n_e \, ldl \tag{2.13}$$

Where

n_e $l = Electron\ density\ along\ the\ signal\ path\ from\ the\ satellite\ to\ the\ reciever$

$l = Signal\ path\ distance\ in\ the\ direction\ from\ the\ satellite\ to\ the\ reciever$

Neglecting higher order terms, the ionosphere delay for the code phase and advance for the carrier phase is given by:

$$I_{PR} = -1_{AD} = \frac{40.3}{f^2} TEC \tag{2.14}$$

TEC is normally measured in TEC Units (TECU), where 1 TECU = $10^{16}\ e/m^2$ and it induces a delay of 0.162 m on L1 signals and 0.267 m on L2 signals. Total Electron Content is a function of time, user location, satellite elevation angle, season, ionizing flux, magnetic activity, sunspot cycle and scintillation. It usually lies in the range of $10^{16}\ or\ 10^{19}\ e/m^2$.

The Total Electron Content value is usually referred to as slant TEC (STEC or just TEC). To map the STEC to the zenith delay or vertical TEC (VTEC), the ionosphere is modelled as a thin shell (Misra and Enge, 2006). A mapping function or obliquity factor

(OF) is introduced in this model to scale STEC to VTEC. The ionospheric OF as a function of elevation angle is defined as follows (Misra and Enge, 2006):

$$OF\ (\theta) = \frac{1}{\sqrt{1-(\frac{R_E cos\theta}{R_E + hl}^2)}} \tag{2.15}$$

where:

$\theta = Elevation\ angle\ at\ the\ user\ location$

$R_E = Average\ earth\ radius\ of\ the\ earth.$

$hl = Mean\ height\ of\ the\ ionospheric\ shell, which\ is\ usually\ taken\ in\ the\ range\ of\ 300 - 400$ Km

Then TEC and VTEC can be related by OF as below:

$$STEC = VTEC\ .OF\ (\theta)$$

The range of OF is from one (zenith direction) to around three for a satellite at an elevation angle of five degrees.

Equation (2.15) can be used to relate ionospheric delay to the ionospheric zenith delay as follow (Misra and Enge, 2006);

$$I(\theta)\ IZ = I\ .OF\ (\theta)$$

$I = ionospheric\ delay$

$IZ = ionospheric\ Zenith\ delay$

For mid latitude locations, IZ is about 1.3 m at night and 5-15 m in the mid-afternoon (around 2 pm at local time) when IZ typically reaches its highest value during the day (,Mistra and Enge, 2006).

Decades of ionospheric research showed that TEC is highly variable and depends on several factors such as local time, geographic location, season and solar cycle (e.g Jakowski, 1996, Jakowski et al., 1999; Tsurutani et al., 2005; Mannucci et al., 2005; Fedrizzi et al., 2005; Moeketesi et al., 2007; and Moeketesi, 2008).

Chauhan et al. (2011) studied the diurnal and seasonal variations of GPS TEC during a low solar activity period as observed at a low latitude station Agra. In the study, a dual frequency (1575.42 and 1227.6 MHz) GPS receiver system (GSV 4004B) was employed at Agra station for measurement of TEC. Diurnal variation in TEC was studied by plotting mass plots of TEC for each months for a period of three years between 01 August 2006 – 31 July 2009. The data during the magnetically quiet period was considered for the study. The result revealed a minimum value in TEC around 0500m hrs LT while day maximum around 1400 hrs LT. Almost similar dirnal pattern was observed for all the months of different seasons. In general, the diurnal variation of TEC show a short lived pre- dawn minimum, a steady early morning increase, followed by an afternoon maximum and gradual fall after sunset. Large variations in TEC were observed in day time, while nightie variations were found to be almost constant. The seasonal variations showed that low values of TEC were observed in winter where as high values were observed in the equinox and summer.

Fayose et al., (2012) studied the Total Electron Content (TEC) over a tropical region in Akure, Nigeria (7.15^0N, 5.12^0E) using GPS data collected over a period of one year. The data was analysed using GPS – TEC analysis application software provided by Institute of scientific research, Boston college, USA. Result obtained shows significant daily and seasonal variation of TEC gradients in the region.

Ezuger et al. (2004) studied the behavior of the vertical Total electron Content obtained from GPS signals, received during the high solar activity year 1999 at 10 stations of the American sector. The considered latitude range extends from 18.4^0N to 64.7^0N and the longitude ranges from 281.3^0 W to 297.7^0 W, the result of this study showed that the VTEC variability during daylight hours is about 30% of median or less and for night time hours is greater than the mentioned percentage, particularly at last hours of the night near the northern peak of the equatorial anomaly. The GPS signals traverse the ionosphere carrying signature of the dynamic medium and offer opportunities for ionospheric research. Global distributions of TEC variations as well as its characteristics at equatorial, middle and high lattitudes have been investigated by a number of workers (Maltseva et al., 2012).

Rama et.al.,(2006) Presented the temporal and spatial variations in TEC derived from the simultaneous and continuous measurements for the first time using the Indian GPS network of 18 receivers located from the equator to the northern crest of the equatorial ionization anomaly (EIA) region and beyond, covering a geomagnetic latitude range 10-24N. In the analysis, they used 16- month data for the low sunspot activity period of March 2004- June 2005. In their findings, along with the diurnal and seasonal variations in TEC, the day to day variability was also significant at all the stations, particularly during the daytime, with maximum variations at EIA crest regions.

Bagiya et al., (2009) Investigated Diurnal and seasonal variations of TEC during low solar activity period (2005-2007) at Rakjot, a station near the equatorial ionization anomaly crest in India. It was found that TEC was maximum during equinoctial months (March, April, September and October) and minimum during winter months (November,

December, January and February), with intermediate values during summer months (May, June, July and August).

Several studies have reported the long-term trends in TEC and its variability over different regions of the ionosphere. Laštovička et al. (2017) reported a positive trend in TEC over the Northern Hemisphere during solar cycle 23. Lean et al. (2016) found a spatial pattern of TEC variability with higher TEC values over the equatorial region and lower values over high latitudes. Zhang et al. (2011) investigated the impact of solar flares on TEC in the equatorial region of the ionosphere. The authors used data from the Chinese Meridian Project Array and found that the TEC increased significantly following solar flares. The authors concluded that the ionospheric response to solar flares was dependent on the location, magnitude, and duration of the flares. Lean et al. (2011) studied the global and hemispheric climatology of TEC using data obtained from the Defense Meteorological Satellite Program. The authors observed a strong correlation between TEC and solar activity, with TEC increasing during periods of high solar activity. The authors also found that the TEC was higher in the summer hemisphere than in the winter hemisphere and was lower at mid-latitudes than at the equator. Cesaroni et al., (2015) also investigated the relationship between TEC and solar ionizing indices and reported a strong correlation between TEC gradients and L-band scintillations during the last solar maximum. Zhang (2016) proposed three methods to retrieve slant TEC measurements from ground-based GPS receivers and assessed their performance. These studies provide insights into the methods of TEC retrieval and the relationship between TEC and other ionospheric parameters.

CHAPTER THREE

3.0 DATA AND METHOD OF ANALYSIS

3.1 DATA

The GNSS observation data in Receiver Independent Exchange (RINEX) format for the representative months of January, March, June, September and December (1996-2008). Were obtained for Total Electron Content (TEC) data: Global ionospheric maps (GIMs) published by IGS can provide TEC data worldwide. At present, IGS has more than 500 global navigation satellite system (GNSS) sites distributed worldwide. TEC values will be retrieved from the downloaded Global Ionospheric Map files for a complete solar cycle 23 which were obtained from the server based gnsss website (see the link) **(www.https://Cddis.nasa.gov/product/archive/gnss).**

3.2 METHOD OF ANALYSIS

Vertical electron content (VTEC) values were obtained using software developed by Gopi Krishma Samela (Gopi, 2012). The input files to the software are the observation and navigation files while the output files are .STD and .CMN. The .CMN files are used for this study. The .CMN files contain both the STEC's and VTEC's over the ionospheric pierce point (IPP). In Gopi, 2012, VTEC values are obtained from STEC's using equation (3.1).

$$V_{TEC} = (TEC_{sl} - bs - br)\cos[\left(arcsin\frac{R_E\, cos\alpha}{R_E + h}\right)] \quad (3.1)$$

Where the parameters are defined as follows:

$TEC_{sl} = Slant\ path\ TEC$

$b_r = Reciever$ biases

$b_s = Satellite\ \ biases$

$R_E = 6378\ km$

$h = Height\ of\ the\ Ionospheric\ layer$

$\alpha = Elevation\ angle\ of\ the\ satellite$

The cut-off elevation angle, 30°, is selected to reduce the time shift and to avoid unnecessary errors caused by multipath and uncertain number of data. Pseudo-range with low elevation is more likely to be affected by the multipath effect and the decrease in reliability than that with high elevation. If the elevation angle is too high, a few satellites will record data to the ground-based GPS receiver, resulting in the decline in the measured data. TEC_{sl} which is calculated from the pseudo ranges (P1 and P2), and the phases (L1 and L2) of the two signals, is given by (Liu, Huang et al. 2012).

Equation (3.1) and (3.2) are the absolute and relative values of $TEC_{sl.}$. To obtain high accuracy for TEC_{sl}, a parameter named B_{rs} baseline is introduced. This parameter is computed as the average difference between TEC_{slpi} and TEC_{slli} from i=1 to i=N. B_{rs} is defined as follows (Liu, Huang et al. 2012).

$$TEC_{sll} = \frac{(f_1 f_2)^2}{40.31\ ((f_1^2 - f_2^2)}\ (l_1\lambda_1 - l_2\lambda_2) \quad (3.2)$$

where

$$TEC_{slp} = \frac{f_1 f_2}{40.31(f_1^{\,2} - f_2^{\,2})}(p_2 - p_1) \quad (3.3)$$

$\lambda_1 = The\ wavelength\ that\ corresponds\ to\ f_1$

$\lambda_2 = The\ wavelengths\ that\ corresponds\ to\ f_2$

Reliance of modern community on navigation and communication system such as GPS since the late 1980s led to formal recognition of the International GPS Service (IGS) and IGS has become an important source for observing the TEC in almost real-time. The data of two receiver stations used for this investigation were obtained from the IGS web server. In this work, the obtained results used universal time (UT) zone in which for the equatorial station, its LT is 1 hour ahead from UT, The IGS is a voluntary federation of more than 200 agencies that pool resources and permanent GPS and GLONASS station data to generate precise GPS and GLONASS products (http://igscb.jpl.nasa.gov). These data are accessible from several servers including at the Crustal Dynamics Data Information System (CDDIS) server (ftp://cddis.gsfc.nasa.gov/pub/gps/data/daily/). GPS measurements based on dual-frequency signals $f1$, (1575.42 MHz) and $f2$, (1227.60 MHz), were used to obtain the vertical TEC data in 2008 and 2013 for the stations. The ground-based dual-frequency GPS receiver constantly records the two pseudo-ranges (P1 and P2) and the phases (L1 and L2) of the two signals. The obtained data were used to estimate the slant TEC, STEC at 30 s interval and to calculate vertical TEC, VTEC (Ma and Maruyama 2003). The vertical TEC is the total number of electrons in a vertical column with a cross sectional area of 1 m2 along the ray path (Klobuchar, 1996). In practice, VTEC is given by (Liu, Huang et al. 2012).

$$B_{rs} = \sum_{i-1}^{N} \frac{(TEC_{slpi} - TEC_{slli}) sin^2 \alpha_1}{\sum_{i=1}^{N} sin^2 \alpha_1} \quad (3.4)$$

where B_{rs} = baseline

$N = Number\ of\ measurements\ transmitted\ by\ the\ satellite$

$sin^2 \alpha_1 = Weighting\ factor$

$Sin^2\ \alpha i$ is used to reduce the multipath effect. TEC_{sll} is fitted to TEC_{slp} then the slant TEC_{sl} is

obtained by (Liu, Huang et al. 2012)

$$TEC_{sl} = TEC_{sll} + B_{rs} \quad (3.5)$$

Data retrieved from IGS network are stored in the Receiver Independent Exchange (RINEX) observation files. The GPS RINEX observation files are processed using Equation (3.1) to (3.5) in the GPS-TEC analysis application software version 2.5, developed by Gopi Seemala of the Institute for Scientific Research, Boston College, USA (Olawepo, Oladipo et al. 2015). The program plots vertical TEC on the screen and writes ASCII output files such as *.CMN and *.STD files. These files are required to represent data results in graphical form. In this study, the GPS observation data in 1998 - 2008 for the stations are processed. The respective RINEX observation files data of 1998 – 2008 were processed for further TEC analysis. In order to gain comprehensive results, the obtained TEC values are represented in graphical form by using Excel for data computation and plotting.

The data collected would be analyzed across different latitudinal TEC values, geographic coordinates to determine the trends and patterns of the ionospheric parameters under investigation. The correlation analysis will be conducted separately for the equatorial,

mid-latitude, and high-latitude regions of the ionosphere. The data will be segregated based on the latitudinal position of the stations which will facilitate the comparison of the correlation trends across different regions. The results will be presented in tables, graphs, and statistical summaries, which would be used for the interpretation of the results.

CHAPTER FOUR

4.1 RESULTS

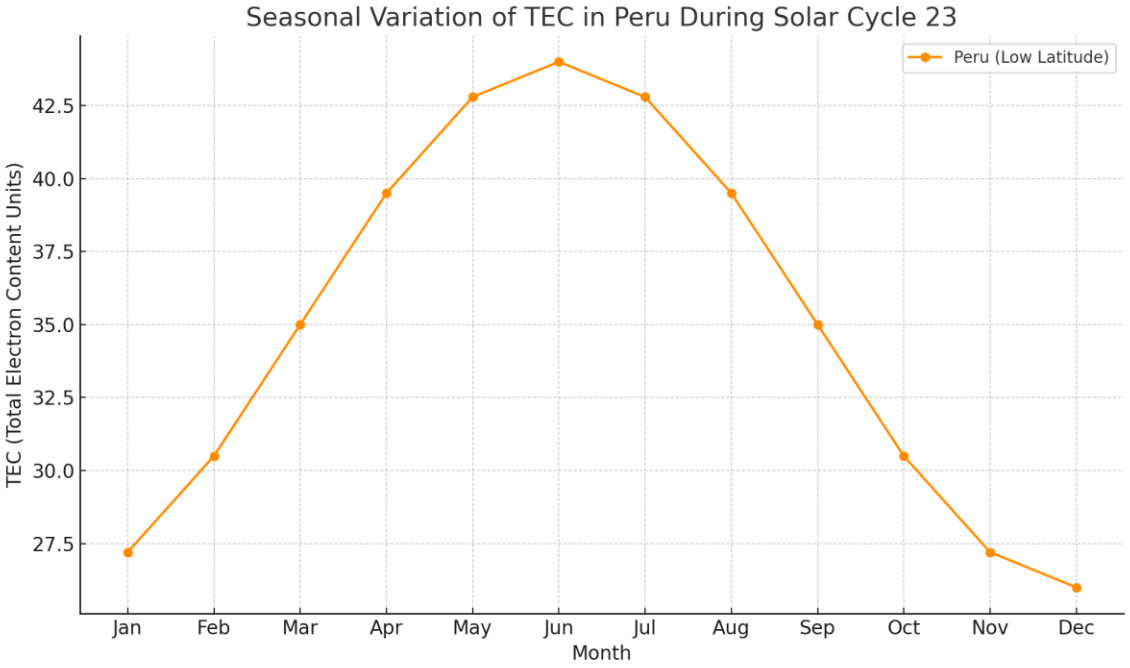

Figure 4.2: Seasonal Variation of Total Electron Content (TEC) in Peru during Solar Cycle 23.

4.2 DISCUSSION

4.2.1 Seasonal Variation of TEC in the Low-Latitude Ionosphere Over Peru and the Marshall Islands During Solar Cycle 23

The ionosphere over low-latitude regions such as Peru and the Marshall Islands exhibits significant seasonal variation in Total Electron Content (TEC), largely influenced by solar radiation, geomagnetic field configuration, and equatorial electrodynamics. Throughout Solar Cycle 23 (1996–2008), a distinct semi - annual pattern in TEC was observed at these locations, modulated by the level of solar activity and seasonal changes

in ionospheric dynamics. Both Peru and the Marshall Islands lie within the equatorial and low-latitude ionospheric region, where TEC is strongly governed by the equatorial fountain effect. This process, driven by the eastward electric field and daytime solar heating, lifts plasma at the magnetic equator via vertical E×B drift. The plasma then diffuses along magnetic field lines, forming the Equatorial Ionization Anomaly (EIA) with two crests of enhanced TEC located about ± 15° from the magnetic equator.

Seasonally, TEC over these stations typically peaks during the equinox months (March and September) and reaches minima during the solstices (June and December). This equinoctial maximum is attributed to nearly overhead position of the Sun at the equator, enhancing photoionization, more symmetric geomagnetic conditions that optimize plasma uplift and transport and minimal disruption from seasonal neutral wind patterns.

During equinoxes, the vertical plasma drift is strongest, resulting in enhanced plasma redistribution and elevated TEC at both stations. In contrast, during the solstices, the ionospheric response weakens due to changes in thermospheric winds and solar zenith angle, leading to reduced TEC.

Despite their similar latitudinal classification, regional differences such as geomagnetic declination and longitude-driven electrodynamic variations can cause slight differences in TEC magnitude and the timing of seasonal peaks between Peru and the Marshall Islands. However, the overall seasonal trend remains consistent across both stations. Importantly, the amplitude of seasonal TEC variation was found to be significantly higher during the

solar maximum years (1999–2002), due to increased solar EUV radiation and stronger ionospheric heating. Conversely, solar minimum periods (1996–1997, 2007–2008) were characterized by reduced TEC levels and weaker seasonal contrasts.

CHAPTER FIVE

5.0 CONCLUSION

The seasonal variation of Total Electron Content (TEC) in the low-latitude ionosphere over Peru and the Marshall Islands during Solar Cycle 23 is characterized by prominent equinoctial maxima and solstitial minima. This pattern reflects the dominant influence of solar radiation, the equatorial fountain effect, and electrodynamic processes on ionospheric behavior at low latitudes. Despite slight regional differences, both stations exhibit similar trends driven by enhanced vertical plasma drifts during equinoxes and diminished ionospheric activity during solstices. These findings underscore the critical role of seasonal and solar cycle modulations in shaping ionospheric conditions, with significant implications for GNSS reliability and space weather forecasting in equatorial regions.

REFERENCES

Abdu, M. A., "Outstanding problems in the equatorial ionosphere – thermosphere Electro-dynamics relevant to spread F, J. Atmos. & Sol. Terr. Phys., 63, 2001, 869- 884.

Bagiya, M.S.; Joshi H.P.; Iyer K.N.; Aggarwal M.;Ravindran S.; Pathan B.M. (2009) TEC variations during low solar activity periods (2005- 2007) near the equatorial ionospheric anomaly crest region in india, Ann Geophysical (Germany), v. 27, p 1047-1057.

Batista, I.S and Abdu, M.A., (2004), Ionospheric variability at Brazilian low and equatorial latitudes comparison between observations and IRI model. Journal of Adavances I space Research v.34 p. 1894-1894.

B. Mangla, "Study of ionic behavior of ionosphere F2 region using satellite data," Thesis, Mirror Shodhganga, 2018, http://hdl. handle.net/10603/214144.

B. Rathore, D. Gupta, and K. Parashar, "Relation between Solar Wind Parameter and Geomagnetic Storm Condition during Cycle-23," International Journal of Geosciences, 10.4236/ijg.2014.513131. 2014, Vol. 05. pp. 1602-1608,

B. T. Tsurutani, W. D. Gonzalez, G. S. Lakhina and S. Alex, " The extreme magnetic storm of 1- September 1859," J. Geophys. Res, Vol. 108, 2003, pp. 1268.

C. A. Loewe and G. W. Prolss, "Classification of mean behavior of magnetic storms," Journal of Geophysical Research, Vol. 102(A7), 1997, pp. 14, 209 14,213,

C. E. Valladares, R. Sheehan, J. Villalobos (2004). Latitudinal network of GPS receivers dedicated to studies of equatorial spread *F* first published: 12 February 2004 https://doi.org/10.1029/2002RS002853

Chakrabarty A D, M.S. Bagiya, S.V Thampi, and K.N, Iyer (2002), Solar EUV flux (0.1-5.0nm), F10.7cm flux, sunspot number and total electron content in the crest region of the ionization anomaly during the deep minimum between solar cycle 23 and 24, Indian J. Radio and Space Physics. 41, 26 -36.

Doschek, G., & Tanaka, K. (1987). Transient ionization and solar flare X-rayspectra. The Astrophysical Journal, 323, 799 – 809.

D. K. Sharma., J. Rai, M. Israil and P. Subrahmanyam,"Diurnal, seasonal and latitudinal variation of ionospheric temperatures of the topside F region over Indian region during solar minimum year 1995-96," J. Atmos. Solar-Terr. Phys, Vol. 67, 2005, pp. 269-274

Florida, 1988. K. Davies, "Ionospheric Radio", Institution of Engineering and

Technology, London, U. K., Vol. 31, 1990.

Forbes J M, Palo S E and Zhang X 2000 Variability of the ionosphere; J. Atmos. Sol.-Terr. Phys. 62 685–693.

Gallileo (2005). Mission High level Definition (HLD) (2002). European commission Communication Document, W. Doc. 2002/05, Version 3, 23. Retrieved From http://www. Galileoju,com issue 5-Rev

Gopi, S (2012). RINEX GPS – TEC program version 2.2.0 Boston college.

Güyer, Sinan & Can, Zehra, "Solar flare effects on the ionosphere". RAST 2013 – Proceedings of 6th International Conference on Recent Advances in Space Technologies, 2013, pp.729-733, 10.1109/RAST.2013.6581305.

H. Rishbeth and O. K. Garriott, "Introduction to ionospheric physics," 1st ed., Academic Press, New York, Vol. 47, pp. 234, 1969.

Jefrey M. Forbes, Scott E. Palo, Xiaoli Zhang (1999)."Variability of the ionosphere" Department of Aerospace Engineering Sciences, Campus Box 429, University of Colorado, Boulder, CO 80309-0429, USA Received 30 August 1999; accepted 10 November 1999

J. Rai, M. Rao, and B.A. P. Tantry, "Bremsstrahlung as a Possible Source of UHF Emissions from Lightning," Nature Physical Science., Vol. 238, 1972.

K. Davies, "Ionospheric Radio", Institution of Engineering and Technology, London, U. K., Vol. 31, 1990.

Kane R P 1980 Irregular variations in the global distribution of total electron content; Radio Sci. 15 837–842.

K. F. Tapping, "The 10.7 cm solar radio flux (F10.7)," Space Weather, Vol. 11, 2013, pp. 394-406, 10.1002/swe.20064.

L. F. McNamara, "The Ionosphere: Communications, Surveillance, and Direction Finding," Krieger, Malabar, Fla., 1991.

M. A. Abdu, I. S. Batista, H. Takahashi, J. MacDougall, J. H. Sobral, A. F. Medeiros, and N.B.Trivedi, "Magnetospheric disturbance induced equatorial plasma bubble development and dynamics: A case study in Brazilian sector," J. Geophys. Res., Vol. 108(A12), 2003, pp.1449, doi:10.1029/2002JA009721.

M. A. Abdu, "Major phenomena of the equatorial ionosphere thermosphere system under disturbed conditions," J. Atmos. Terr. Phys., Vol. 59, 1997, pp. 1505-1519.

M. C. Kelley, "The Earth's Ionosphere: Plasma Physics and Electrodynamics, Academic, San Diego, Calif., 1989.

N. Bergeot, Juliette Legrand and Robert Burston (2010). Correlation between solar activity and Earth's ionospheric electron content during the 23rd solar cycle. https://www.researchgate.net/publication/252693909

Olawepo, A. O., Oladipo, O. A., Adeniyi, J. O. and Doherty, P. H.,TEC response at two equatorial stations in the African sector to geo-magnetic storms. Adv. Space Res., 2015, 56(1), 19–27.

R. G. Rastogi, J. A. Klobuchar (1990). Ionospheric electron content within the equatorial F2layer anomaly belt first published: 1 November 1990 https://doi.org/10.1029/JA095iA11p19045

T. F. Tascione, "Introduction to the Space Environment", Orbit Book Company Inc., Malabar, Florida, 1988.

V. Depuev and T. Zelenova, "Electron density profile changes in a pre-earthquake period," Advances in Space Research, Vol. 18, 1996, pp.115-118.

W. D. Gonzalez, J. A Joselyn, Y. Kamide, H. W. Kroehl, G. Rostoker, B. T Tsurutani, V. M. Vasyliunas, "What is a geomagnetic storm," Journal of Geophysical Research, Vol. 99, 1994, pp. 5771–5792, 92

W. D Gonzalez, B. T. Tsurutani, and A. L. Clua de Gonzalez, "Interplanetary origin of magnetic storms," Space Sci. Rev., Vol. 88, 1999, pp. 529– 562.